Journal of Alloys and Compounds 506 (2010) 698–702

Contents lists available at ScienceDirect

Journal of Alloys and Compounds

journal homepage: www.elsevier.com/locate/jallcom

Sol–gel synthesis of Pt-Ru-Os-Ir based anode electro-catalysts for direct methanol fuel cells

Yousef M. Alyousef[a], Moni Kanchan Datta[b], Karan Kadakia[c], S.C. Yao[d], Prashant N. Kumta[b,c,e,*]

[a] Energy Research Institute, King Abdulaziz City for Science and Technology, Riyadh 11442, Saudi Arabia
[b] Department of Bioengineering, Swanson School of Engineering, University of Pittsburgh, Pittsburgh, PA 15261, United States
[c] Chemical and Petroleum Engineering, Swanson School of Engineering, University of Pittsburgh, Pittsburgh, PA 15261, United States
[d] Department of Mechanical Engineering, Carnegie Mellon University, Pittsburgh, PA 15213, United States
[e] Mechanical Engineering and Materials Science, Swanson School of Engineering, University of Pittsburgh, Pittsburgh, PA 15261, United States

ARTICLE INFO

Article history:
Received 18 March 2010
Received in revised form 7 July 2010
Accepted 7 July 2010
Available online 15 July 2010

Keywords:
Direct methanol fuel cells
Nanostructured materials
Sol–gel process
Electro-catalyst
Metal and alloys

ABSTRACT

A high specific surface area (~95 m^2/g) $Pt_{44}Ru_{41}Os_{10}Ir_5$ based anode electro-catalysts for direct methanol fuel cell, synthesized by a novel complexed sol–gel (CSG) process, shows better catalytic activity in comparison to pure equi-atomic compositions of Pt-50 at.% Ru anode catalysts synthesized by similar sol–gel processes. A homogeneous amorphous gel was successfully synthesized by complexing platinum(II) acetylacetonate, ruthenium(III) acetylacetonate, iridium(III) acetylacetonate and osmium(III) chloride with tetramethylammonium hydroxide (TMAH) used as a complexing agent. Phase-pure Pt(Ru,Os,Ir) and Pt(Ru) solid solutions possessing high specific surface area (SSA) (~90–120 m^2/g) were successfully synthesized by thermal decomposition of the amorphous gel followed by controlled removal of carbonaceous species present in the thermally treated powders. The controlled removal of carbon, present in the thermally treated Pt-Ru-Os-Ir powder, has been successfully achieved by conducting precise thermal treatments of the thermally treated powders using controlled oxidizing atmospheres. Results indicate that the nano-crystalline pure Pt(Ru,Os,Ir) solid solution of nominal composition Pt-41 at.%Ru-10 at.%Os-5 at.% Ir possessing good chemical homogeneity exhibit excellent catalytic activity, demonstrating the potential of the novel complexed sol–gel process for synthesizing high-performance Pt-Ru-Os-Ir based catalysts for direct methanol fuel cells.

1. Introduction

Direct methanol fuel cells (DMFC) are of interest as suitable power sources for several portable electronic devices such as cellular phones, PDA, camcorder and notebook PC [1–4] as well as remote and auxiliary power units for transportation [5,6]. The main advantage of DMFC is the use of liquid methanol rather than gaseous hydrogen as the operating fuel and its operation at low working temperatures. The theoretical energy density afforded by methanol which is in essence, the amount of energy contained in a given volume of methanol is an order of magnitude greater than even highly compressed hydrogen [6] and five to ten times greater than rechargeable lithium ion batteries [1,2]. However, the currently achieved power densities of DMFC are still significantly below that of hydrogen fueled PEM and other fuel cell types which severely limits its use for commercial application. This mainly arises due to the relatively sluggish kinetics of the electrochemical reactions occurring on the catalyst layers at the electrode surface combined with the methanol crossover to the cathode compartment [1,3,6–9]. There is therefore a critical need to conduct research and develop new and improved electro-catalysts with higher catalytic activity at both the anode and cathode regions in order to enhance the efficiency and power density of DMFC, while lowering the precious metal loadings necessary to realize the much-desired cost savings to match the performance. Currently, Pt-Ru alloy of nominal composition Pt-50 at.% Ru is considered the most suitable electro-oxidation catalyst composition for oxidation of methanol yielding the best catalytic activity and is hence widely recognized as the effective anode catalyst for use in DMFCs to date [3,6,7,10–14].

Improved anode catalysts can be obtained by synthesizing high surface area Pt-Ru based alloy catalysts combined with engineered proper alloy design by modifying the chemical composition of the alloy, and doping or alloying with other elements onto the catalyst structure [3,7,10–18]. Several researchers have reported significantly improved performance in ternary and quaternary alloys of Pt-Ru-Os, Pt-Ru-Ir, Pt-Ru-Sn, Pt-Ru-Ni, Pt-Ru-P, Pr-Ru-Ni-Zr, Pt-Ru-Os-Ir etc. when compared to pure Pt-Ru alloys [14–20]. Out of the different multi-component systems, it has been reported that Pt-Ru-Os and Pt-Ru-Os-Ir exhibit superior catalytic activity

---

* Corresponding author at: Department of Bioengineering, Swanson School of Engineering, 848 Benedum Hall, 3700 O'Hara Street, University of Pittsburgh, Pittsburgh, PA 15261, United States.
E-mail address: pkumta@pitt.edu (P.N. Kumta).

0925-8388/$ – see front matter © 2010 Elsevier B.V. All rights reserved.
doi:10.1016/j.jallcom.2010.07.046

in comparison to other systems [14–16,22,23]. Reddington et al. [15,22] and Chu and Jiang [14] have reported that Pt-Ru-Os and Pt-Ru-Os-Ir based catalysts of specific surface area ~31 m^2/g show better catalytic activity in comparison to Pt-Ru alloy despite the higher specific surface area of the latter (~65 m^2/g). In recent years, we have also reported the improved catalytic activity of phase-pure Pt-Ru-Os alloy with respect to Pt-50 at.% Ru alloy of comparable specific surface area [16]. Using combinatorial electrochemistry of five elements (Pt, Ru, Os, Ir and Rh), Reddington et al. [15] has reported that the electro-catalyst of nominal composition $Pt_{44}Ru_{41}Os_{10}Ir_5$ is more active than $Pt_{50}Ru_{50}$ in a direct methanol fuel cell operating at 60 °C, even though the latter catalyst has about twice the surface area of the former. Synthesis of nano-crystalline $Pt_{44}Ru_{41}Os_{10}Ir_5$ catalyst of high specific surface area as reported herein can therefore be expected to enhance the catalytic activity in comparison to high surface area $Pt_{50}Ru_{50}$ alloy. Furthermore, an SEM–EDAX analysis of commercially obtained Pt-Ru based Johnson-Matthey (JM) catalyst showed presence of Os which also served as a motivation for the incorporation of Os and Ir in the present work. In addition to alloy development, considerable efforts have also been devoted to synthesize high surface area binary or ternary Pt-Ru based alloy catalysts to achieve higher methanol oxidation activity [7,10–13,20–25]. Hence, several approaches have been reported for synthesizing high surface area Pt-Ru based binary or ternary alloy nano-particles anode catalysts primarily using halide precursors of the respective components, which inevitably require several follow-up washing treatments to remove the undesired halide secondary residues [7,10–21]. As a result, these processes are cumbersome and cost-inefficient leading to significant loss of the starting noble metal precursors. In addition, the use of Vulcan carbon and other high surface area electronic conductors (e.g. carbon nanotube and metal oxide) have been reported as supports to synthesize high surface area Pt-Ru based anode catalyst to obtain better performance than pure Pt-Ru catalyst [7,11,12,18,20,24–26]. However, the relatively low density of carbon leads to a build-up of thick catalyst layers that impede the mass transport of methanol to the catalytic sites.

We have demonstrated that the novel sol–gel complexation based chemical process, aptly termed complexed sol–gel (CSG) process, is an attractive alternative route for synthesizing unsupported phase-pure Pt(Ru) and Pt(Ru,Os) solid solution catalyst possessing a high specific surface area (>100 m^2/g) with excellent catalytic activity [13,16,27]. In the present work, the CSG process has been further exploited to synthesize $Pt_{44}Ru_{41}Os_{10}Ir_5$ based complexes, which were thermally treated at various conditions to synthesize phase-pure Pt(Ru,Os,Ir) solid solution catalysts possessing a high specific surface area (SSA) with good catalytic activity. The synthesis, phase analysis, thermal characteristics, and electrochemical performance of the high specific surface area $Pt_{44}Ru_{41}Os_{10}Ir_5$ catalyst is presented and described in the present manuscript.

2. Experimental details

2.1. Materials synthesis

Phase-pure and high specific surface area (SSA) Pt-Ru-Os-Ir based catalyst powders were synthesized using the CSG process. Platinum(II) acetylacetonate [Pt-acac: $Pt(C_5H_7O_2)_2$, Alfa Aesar], ruthenium(III) acetylacetonate [Ru-acac, $Ru(C_5H_7O_2)_3$, Alfa Aesar], iridium(III) acetylacetonate [Ir-acac, $Ir(C_5H_7O_2)_3$, Alfa Aesar] and osmium(III) chloride [$OsCl_3$, Sigma–Aldrich] were used as the sources for Pt, Ru, Ir and Os. Pt-acac, Ru-acac, Ir-acac and $OsCl_3$ of the desired composition (e.g. Pt-41 at.%Ru-10 at.%Os-5 at.%Ir) were dissolved at 50 °C in 100 ml of acetone. Tetramethylammonium hydroxide [TMAH, $(CH_3)_4NOH$, 25% in methanol, Alfa Aesar], set at TMAH:(Pt + Ru + Os) = 1.75:1, was then added to the solution to serve both as a high molecular weight organic complexing as well as a hydrolyzing agent. Since Pt-acac, Ru-acac, Ir-acac and $OsCl_3$ tend to phase separate during drying and evaporation of the solvent, the addition of the high molecular weight organic reagent, tetramethylammonium hydroxide (TMAH), and its intended dual role to complex and induce hydrolysis of the starting noble metal precursors was found to be beneficial in yielding homogeneous amorphous gels containing Pt, Ru, Ir and Os. After stirring for 10 min, the solvent was evaporated until the solution became viscous, transforming into a thixotropic gel. The viscous gel was dried in air at 120 °C for 10 h. The dried gels were then heat-treated in various conditions based on our earlier published results [13,16,27] to generate high surface area Pt-Ru-Os-Ir catalysts. In order to compare the electrochemical performance of the Pt-Ru-Os-Ir catalyst with Pt-Ru catalyst, the CSG process has also been used to synthesize high specific surface area Pt-50 at.% Ru alloy as reported by us previously [13,16,27].

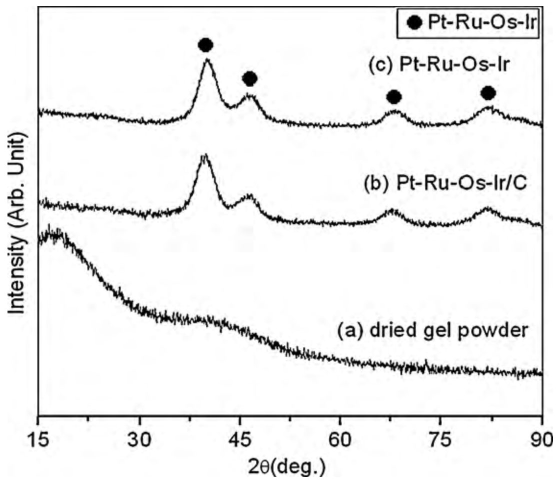

Fig. 1. X-ray diffraction traces of the Pt-Ru-Os-Ir based alloy powders derived using tetramethylammonium hydroxide (TMAH) acting as a hydrolysis and a complexing agent; (a) dried gel powder obtained after drying the gel precursor at 120 °C for 10 h in air, (b) Pt-Ru-Os-Ir/C obtained after thermal treatment of the dried gel powder in UHP–Ar at 450 °C for 4 h, (c) Pt-Ru-Os-Ir alloy obtained after two sequential thermal treatment cycles of Pt-Ru-Os-Ir/C at 300 °C in Ar-1% O_2 atmosphere for 3 h.

2.2. Materials characterization

In order to identify the presence of phase/phases, X-ray diffraction (XRD, Philips XPERT PRO system with CuKα radiation) study has been conducted on the as-prepared precursors as well as the heat-treated powders. The effective crystallite sizes of the Pt-Ru and Pt-Ru-Os-Ir catalysts were calculated from the most intense peak by Voigt function using the single line approximation method [28]. Specific surface area of the catalyst has been measured using the Brunauer–Emmett–Teller (BET) technique (ASAP 2020 Accelerated Surface Area and Porosimetry System, Micromeritics). In order to understand the phase formation and decomposition temperature, thermogravimetric and differential scanning calorimetry (TGA/DSC) has been conducted on the as-prepared precursors as well as the thermally treated powders using a simultaneous TGA/DSC machine (STA 409PC Luxx, Netzsch). The TGA/DSC analysis has been carried out employing a heating rate of 10 °C/min from room temperature to 500 °C in various atmospheres using ~10 mg sample mentioned in the sections to follow. To investigate the particle size and particle morphology, transmission electron microscopy (TEM) analysis was conducted. JEOL 4000EX operating at 400 kV was employed for conducting the TEM analysis.

Electrochemical characterization was conducted on selected samples using a three-electrode cell. The working electrodes for electrochemical characterization were prepared by spreading the catalyst ink of the respective powders on teflonized carbon papers (applied on 1.5 cm^2 area). The ink consists of 88 wt% catalysts, and 12 wt% Nafion (5 wt% solution in mixed alcohols, Aldrich). The Pt loading on the electrode was 0.2 mg/1.5 cm^2. The working electrodes were electrochemically tested using a Potentiostat/Galvanostat (VersaSTAT 3, Princeton Applied Research). A solution containing 1 M methanol and 0.5 M sulfuric acid was used as an electrolyte while also serving as a source of the fuel. A Mercury/Mercurous sulfate electrode that has a potential of +0.65 V with respect to standard hydrogen electrode (SHE) was used as the reference electrode.

3. Results and discussion

The XRD patterns of the dried gel precursor (Fig. 1a) obtained after drying the as prepared gel, derived using a molar ratio of TMAH:(Pt-acac + Ru-acac + Ir-acac + $OsCl_3$) = 1.75:1 of nominal composition Pt-acac:Ru-acac:$OsCl_3$:Ir-acac = 4.4:4.1:1.0:0.5, at 120 °C for 10 h in air exhibit an amorphous structure devoid of any peaks corresponding to the crystalline starting precursors which indicate the expected good chemical homogeneity of the dried gel

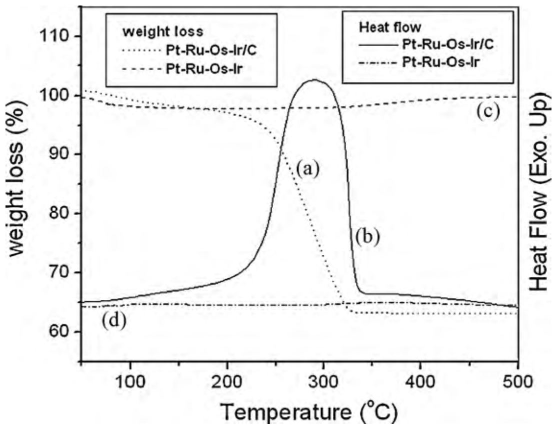

Fig. 2. (a) TGA traces of Pt-Ru-Os-Ir/C in air showing the significant weight loss corresponding to the presence of carbon, (b) DSC traces of Pt-Ru-Os-Ir/C in air confirming the exothermic oxidation of carbon, (c) TGA traces of pure Pt-Ru-Os-Ir in air showing negligible weight loss indicating absence of carbon originally present in the UHP-Ar treated gels, and (d) DSC traces of pure Pt-Ru-Os-Ir alloy powder conducted in air up to 500 °C.

powders due to the possible complexation and hydrolysis of Pt-acac, Ru-acac, Ir-acac and $OsCl_3$ with TMAH. The dried gel powder, obtained after drying the gel precursor at 120 °C for 10 h in air, was heat-treated in various conditions to synthesize nano-crystalline phase-pure Pt(Ru,Os,Ir) solid solution alloys of nominal composition Pt-41 at.% Ru-10 at.% Os-5 at.% Ir. The TGA/DSC analysis of the dried gel powder performed under ultrahigh purity argon (UHP-Ar) atmosphere shows that the decomposition of the dried gel powder is almost complete at around ∼450 °C, consistent with our earlier publications [13,16,27] related to Pt-Ru and Pt-Ru-Os based electro-catalyst systems. Hence accordingly, the dried gel powder of Pt-Ru-Os-Ir system was heat-treated at 450 °C for 6 h under UHP-Ar atmosphere in order to decompose the amorphous gel structure resulting in the formation of nano-crystalline Pt-Ru-Os-Ir based alloys. The XRD patterns of the heat-treated powder (Fig. 1b), obtained after thermal treatment of the dried gel powder at 450 °C for 6 h under UHP-Ar atmosphere, shows the formation of nano-crystalline Pt-Ru-Os-Ir alloy with crystallite size of ∼2–4 nm calculated from the most intense peak using the Voigt function as outlined earlier. However, the presence of large amount of non-conducting carbon (C) has also been detected in the thermally treated Pt-Ru-Os-Ir alloy powders confirmed by the TGA/DSC analysis subsequently conducted on the UHP-Ar treated powders in air (see Fig. 2).

The Pt-Ru-Os-Ir alloy with non-conducting carbon, obtained after thermal treatment of the dried gel powder at 450 °C under UHP-Ar atmosphere, will be thereafter denoted as Pt-Ru-Os-Ir/C. The Pt-Ru-Os-Ir/C obtained after the initial heat treatment in UHP-Ar shows a specific surface area of only ∼8 m^2/g due to the presence of large amount of low surface area non-conducting amorphous carbon (∼40 wt%). The TGA and DSC traces of Pt-Ru-Os-Ir/C up to 500 °C, shown in Fig. 2a and b, respectively, performed under dry air shows the onset of a broad exothermic reaction commencing at temperatures ∼100 °C reaching a maximum at ∼290 °C, and ending at ∼330 °C corresponding to loss of the adsorbed water and the subsequent oxidation reaction corresponding to removal of carbon. This thermal heat flow profile corroborates well with the weight loss events beginning at ∼100 °C corresponding to ∼2% loss of adsorbed water and the enormous weight loss (∼40%) which is expected to arise due to oxidation and elimination of the carbon from Pt-Ru-Os-Ir/C.

In order to remove the carbon related species present in the Pt-Ru-Os-Ir/C alloy to form the desired nano-crystalline phase-pure Pt(Ru,Os,Ir) solid solution alloys with high specific surface area (SSA), the Pt-Ru-Os-Ir/C was further subjected to two sequential thermal treatments at 300 °C for 3 h in the presence of 1% O_2 balanced by UHP-Ar. The 1% oxygen present in UHP-Argon will serve to remove the carbon in a controlled fashion thus yielding the single phase Pt-Ru-Os-Ir alloy, denoted as Pt-Ru-Os-Ir, causing minimal or no significant oxidation of the resulting alloys. The XRD patterns of the resulting Pt-Ru-Os-Ir (Fig. 1c) shows the presence of nano-crystalline Pt-Ru-Os-Ir (∼4 nm) alloy suggesting that there is no significant grain growth occurring during the thermal treatment at 300 °C under Ar-1% O_2 atmosphere while eliminating the undesired non-conducting carbon. In addition, no significant peaks corresponding to crystalline oxides arising as a result of possible oxidation of the metals (e.g. RuO_2, IrO_2, OsO_2 or OsO_4) is observed in the XRD patterns of the resultant Pt-Ru-Os-Ir alloy (Fig. 1c) which suggest that no significant oxidation of resulting alloy occurs during thermal treatment of the Pt-Ru-Os-Ir alloy conducted in Ar-1% O_2 atmosphere up to 300 °C.

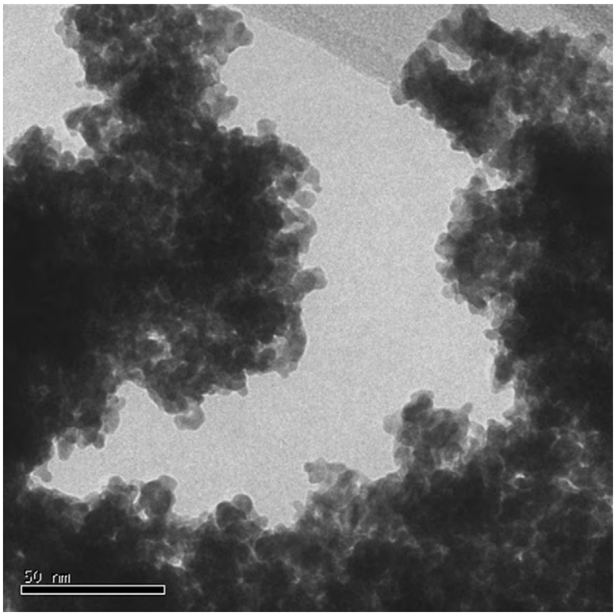

Fig. 3. TEM bright field image shows the formation of nano-particle (∼5-7 nm) Pt-Ru-Os-Ir alloy powder.

The TEM bright field image, shown in Fig. 3, also confirms the formation of nano-particles of the Pt-Ru-Os-Ir alloy of crystallite size of ∼5–7 nm. The TGA of the resultant Pt-Ru-Os-Ir alloy conducted in the presence of dry air up to 500 °C, shown in Fig. 2c, shows that there is no significant reduction in weight of Pt-Ru-Os-Ir alloy in comparison to Pt-Ru-Os-Ir/C (Fig. 2a) which suggest that the carbon content is almost reduced to ∼0 wt.% in comparison to ∼40 wt.% of C originally present in the Pt-Ru-Os-Ir/C obtained after UHP-Ar treatment of the gels. Furthermore, the DSC curve of Pt-Ru-Os-Ir alloy (Fig. 2d) also shows no significant exothermic reaction occurring due to burn off of the carbon, if present, to produce carbon dioxide in the presence of dry air, further confirming the absence of carbon. The above results clearly suggest that the thermal treatment conducted in the presence of Ar-1% O_2 at 300 °C is therefore helpful in removing the non-conducting carbon related species from the Pt-Ru-Os-Ir/C catalyst powders without causing any significant oxidation and grain growth of Pt(Ru,Os,Ir) solid solution. The synthesized Pt(Ru,Os,Ir) solid solution of nominal composition Pt-41 at.%Ru-10 at.%Os-5 at.%Ir obtained after controlled heat treatment in Ar-1% O_2 shows a specific surface area (SSA) of ∼95 m^2/g in comparison to ∼8 m^2/g corresponding to UHP-Ar treated Pt-Ru-Os-Ir/C. This result clearly suggests that the significant removal of

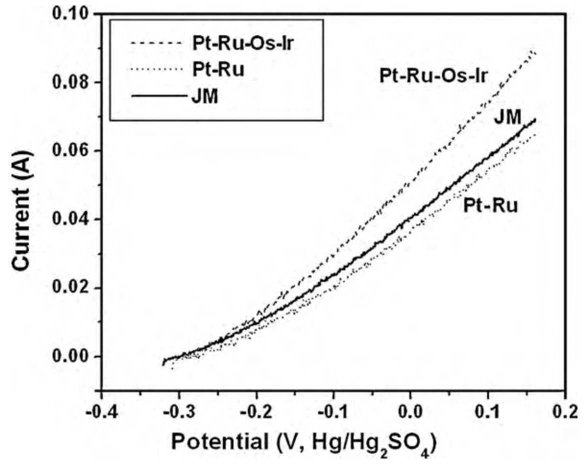

Fig. 4. The polarization curves of Pt-Ru-Os-Ir alloy along with Pt-50 at.% Ru and Johnson-Matthey catalyst tested at 40 °C.

the non-conducting low surface area carbon facilities the formation of a porous structure in the Pt-Ru-Os-Ir alloys while also enhancing the specific surface area. In addition, the removal of carbon also contributes to facilitating the catalytic activity as described in the following.

Results of electrochemical tests, i.e. polarization curve at 40 °C and 60 °C with a Pt loading 0.2 mg/1.5 cm^2, conducted on the Pt-Ru-Os-Ir alloy of specific surface area (SSA) ~95 m^2/g is shown in Figs. 4 and 5, respectively. In order to compare the performance of Pt-Ru-Os-Ir alloy with Pt-50 at.% Ru synthesized by similar CSG processes and also with commercially available Johnson-Matthey catalyst (JM), the electrochemical performance of pure Pt-50 at.%Ru of specific surface area (SSA) ~120 m^2/g and JM catalyst with similar Pt loading (~0.2 mg/1.5 cm^2) is also shown in Figs. 4 and 5. At 40 °C and 60 °C, Pt-50 at.%Ru shows ~0.037 A/1.5 cm^2 and ~0.046 A/1.5 cm^2 current density, respectively at ~0.0 V with respect to Hg/Hg$_2$SO$_4$ reference electrode. The commercially available JM catalyst of surface area (~70 m^2/g) shows comparable performance (~0.040 A/1.5 cm^2 and ~0.045 A/1.5 cm^2 at 40 °C and 60 °C, respectively) with Pt-50 at.% Ru at ~0.0 V. On the other hand, Pt-Ru-Os-Ir shows ~0.052 A/1.5 cm^2 and ~0.062 A/1.5 cm^2 current density, respectively at 40 °C and 60 °C at ~0.0 V, which corresponds to ~35–40% improved performance in comparison to Pt-Ru synthesized via the complexed sol–gel processes and JM catalyst. It has also been identified that the current density of the Pt-Ru-Os-Ir catalyst is 20% higher when the operating temperature is increased from 40 °C to 60 °C. The similar catalytic activity of the Pt-50 at.% Ru with commercially obtained JM catalyst despite the higher specific surface area (SSA ~120 m^2/g) indicate that surface composition and surface structure also contribute to the catalytic activity in addition to the high surface area. This has also been referred to in the earlier reports [10,12,13,16]. Furthermore, as mentioned earlier, the SEM-EDAX analysis of the JM commercial catalyst in fact indicated the presence of Os which motivated the addition of Os in the earlier report [16] and Ir in the present study. Such a modification is indeed achieved by the addition of Osmium and Iridium which indicate a much better electro-catalytic performance compared to the CSG derived Pt-50 at.%Ru as well as the JM catalyst. Attainment of an even higher surface area corresponding to a higher surface activity may be needed to override the surface composition and surface structure dependence. These studies are on going and will be reported in subsequent publications. Thus the above results suggest that the nano-crystalline, high specific surface area, phase-pure Pt(Ru,Os,Ir) solid solution of nominal composition Pt-41 at.% Ru-10 at.% Os-5 at.% Ir with good chemical homogeneity exhibits much improved catalytic activity, demonstrating the potential of the novel complexation based complexed sol–gel (CSG) chemical process for synthesizing high-performance anode catalysts for direct methanol fuel cells.

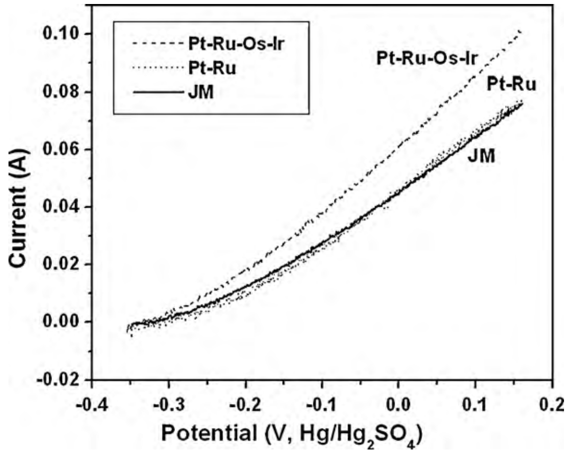

Fig. 5. The polarization curves of Pt-Ru-Os-Ir alloy along with Pt-50 at.% Ru and Johnson-Matthey catalyst tested at 60 °C.

4. Conclusions

A novel complexation based complexed sol–gel (CSG) process has been developed to synthesize Pt-Ru-Os-Ir based anode catalysts possessing high specific surface area (SSA) with good catalytic activity. A homogeneous gel was successfully synthesized by complexing Pt-acac, Ru-acac, Ir-acac and OsCl$_3$ with TMAH serving the dual role of a hydrolysis as well as a complexing agent. Phase-pure Pt-Ru-Os-Ir powders possessing high specific surface area (SSA) ~95 m^2/g was obtained by controlled removal of the non-conducting carbon generated from the thermally decomposed gel precursor in inert atmosphere. The controlled removal of non-conducting carbon has been performed by thermal treatment of carbon containing precursor at 300 °C for 3 h using controlled oxidizing atmospheres such as 1% O$_2$ balanced with UHP-Ar. The electrochemical properties of Pt-Ru-Os-Ir show ~35–40% improved performance in comparison to the equi-atomic pure Pt-Ru alloy of comparable surface area also prepared using the CSG process. It has also been noticed that the catalytic activity of the catalyst increases by 20% when the operating temperature is increased from 40 °C to 60 °C. The above electrochemical test results demonstrate the potential of the novel complexation based sol–gel process utilizing non-halogen precursors of Pt, Ru, and Ir for synthesizing high-performance Pt-Ru-Os-Ir based catalysts for direct methanol fuel cells.

Acknowledgements

The authors would like to acknowledge the financial assistance of King Abdulaziz City for Science and Technology (KACST), Saudi Arabia for supporting this work. Authors also acknowledge the financial support of the Swanson School of Engineering, University of Pittsburgh, and Carnegie Mellon University, while PNK also acknowledges the Edward R, Weidlein Chair Professorship funds for partial support of this research.

References

[1] S.K. Kamarudin, F. Achmad, W.R.W. Daud, Int. J. Hydrogen Energy 34 (2009) 6902–6916.
[2] R. Rashidi, I. Dincer, G.F. Naterer, P. Berg, J. Power Sources 187 (2009) 509–516.
[3] G. Hoogers, Fuel Cell Technology Handbook, CRC press LLC, 2003.

[4] U.A. Icardi, S. Specchia, G.J.R. Fontana, G. Saracco, V. Specchia, J. Power Sources 176 (2008) 460–467.
[5] B.D. McNicol, D.A.J. Rand, K.R. Williams, J. Power Sources 83 (1999) 15–31.
[6] J. Larminie, A. Dicks, Fuel Cell Systems Explained, John Wiley & Sons Ltd., West Sussex, England, 2003, pp: 141–161.
[7] H. Liu, C. Song, L. Zhang, J. Zhang, H. Wang, D.P. Wilkinson, J. Power Sources 155 (2006) 95–110.
[8] E. Antolini, T. Lopes, E.R. Gonzalez, J. Alloys Compd. 461 (2008) 253–262.
[9] C. Xu, A. Faghri, X. Li, T. Ward, Int. J. Hydrogen Energy 35 (2010) 1769–1777.
[10] C. Roth, N. Benker, R. Theissmann, R.J. Nichols, D.J. Schiffrin, Langmuir 24 (2008) 2191–2199.
[11] I.A. Garcia, C. Ramirez, J.M.H. Lopez, E.M.A. Estrada, J. Alloys Compd. 495 (2010) 462–465.
[12] T.Y. Jeon, K.S. Lee, S.J. Yoo, Y.H. Cho, S.H. Kang, Y.E. Sung, Langmuir 26 (2010) 9123–9129.
[13] J.Y. Kim, Z.G. Yang, C.C. Chang, T.I. Valdez, S.R. Narayanan, P.N. Kumta, J. Electrochem. Soc. 150 (2003) A1421–A1431.
[14] D. Chu, R. Jiang, Solid State Ionics 148 (2002) 591.
[15] E. Reddington, A. Sapienza, B. Gurau, R. Viswanathan, S. Sarangapani, E.S. Smotkin, T.E. Mallouk, Science 280 (1998) 1735–1737.
[16] Y.M. Alyousef, M.K. Datta, S.C. Yao, P.N. Kumta, J. Phys. Chem. Solids 70 (2009) 1019–1023.
[17] Q. Yi, L. Li, W. Yu, Z. Zhou, X. Liu, G. Xu, J. Alloys Compd. 466 (2008) 52–58.
[18] J. Liu, J. Cao, Q. Huang, X. Li, Z. Zou, H. Yang, J. Power Sources 175 (2008) 159–165.
[19] J.F. Whitacre, T. Valdez, S.R. Narayanan, J. Electrochem. Soc. 152 (2005) A1780–A1789.
[20] W.D. King, J.D. Corn, O.J. Murphy, D.L. Boxall, E.A. Kenik, K.C. Kwiatkowski, S.R. Stock, C.M. Lukehart, J. Phys. Chem. B 107 (2003) 5467–5474.
[21] J.H. Choi, K.W. Park, B.K. Kwon, Y.E. Sung, J. Electrochem. Soc. 150 (2003) A973–A978.
[22] B. Gurau, R. Viswanathan, R. Liu, T.J. Lafrenz, K.L. Ley, E.S. Smotkin, E. Reddington, A. Sapienza, B.C. Chan, T.E. Mallouk, S. Sarangapani, J. Phys. Chem. B 102 (1998) 9997–10003.
[23] K.L. Ley, R. Liu, C. Pu, Q. Fan, N. Leyarovska, C. Segre, E.S. Smotkin, J. Electrchem Soc. 144 (1997) 1543–1548.
[24] C. Zhou, H. Wang, F. Peng, J. Liang, H. Yu, J. Yang, Langmuir 25 (2009) 7711–7717.
[25] C. Yang, D. Wang, X. Hu, C. Dai, L. Zhang, J. Alloys Compd. 448 (2008) 109–115.
[26] W. Li, X. Wang, Z. Chen, M. Waje, Y. Yan, J. Phys. Chem. B 110 (2006) 15353–15358.
[27] M.K. Datta, J.Y. Kim, P.N. Kumta, Ceram. Trans. 179 (2006) 165–172.
[28] T.H. de Keijeer, J.I. Langford, E.I. Mittemeijer, A.B.P. Vogels, J. Appl. Crystallogr. 15 (1982) 308–314.